Submitted to the 30th International Conference on High-Energy Physics ICHEP2000,
Osaka, Japan, July 2000

A Search for Leptoquark Bosons in e^-p Collisions at HERA

H1 Collaboration

Abstract

A search for scalar and vector leptoquarks (LQs) coupling to first generation fermions is performed in the H1 experiment at the ep collider HERA. The analysis uses all available e^-p data collected in 1998 and 1999 at a centre of mass energy of $\sim$ 320 GeV, corresponding to an integrated luminosity of ~ 14.4 pb $^{-1}$. No evidence for the direct production of such particles is found in the high Q^2 neutral current deep-inelastic scattering data sample, and constraints on LQs are obtained. For a Yukawa coupling of electromagnetic strength LQs are excluded for masses up to $\sim$ 290 GeV. This analysis complements the LQs searches performed previously using data collected while HERA was operating with positrons instead of electrons.

Abstract: 954
Parallel Session: 11
Plenary Talk: 7

1 Introduction

The ep collider HERA offers the unique possibility to search for s-channel resonant production of new particles which couple to lepton-parton pairs. Examples are leptoquark (LQ) colour triplet bosons which appear naturally in various unifying theories beyond the Standard Model (SM). At HERA, leptoquarks could be singly produced by the fusion of the 27.5 GeV initial state lepton with a quark of the 920 GeV incoming proton, with masses up to the kinematic limit of $\sqrt{s_{ep}} \simeq 320$ GeV.

This analysis presents a search for LQs using e^-p data collected in 1998 and 1999. Collisions between *electrons* and protons provide a high sensitivity to LQs coupling to e^- and a *valence quark* (i.e. LQs with fermion number $F = 2$) while the production of such LQs is largely suppressed in e^+p collisions where an *antiquark* should participate to the fusion. Thus this analysis complements the searches for LQs in e^+p data published recently [1].

The search is restricted to the neutral current (NC) decay mode of the LQ which leads to final states similar to those of deep-inelastic scattering (DIS) at very high squared momentum transfer Q^2. The luminosity amounts to 14.41 pb $^{-1}$, an increase in statistics of a factor ~ 35 compared to previous LQs searches [2] in e^-p collisions.

2 Leptoquark Phenomenology

The phenomenology of LQs at HERA is presented in detail in [1]. At HERA, LQs can be resonantly produced in the s-channel or exchanged in the u-channel between the incoming

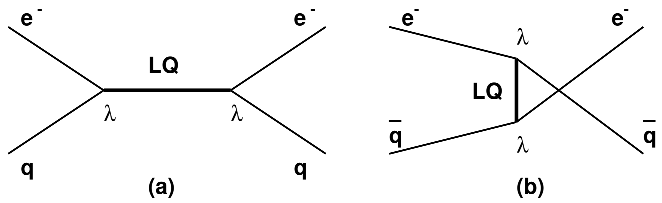

Figure 1: Diagrams (a) s-channel resonant production and (b) u-channel exchange of a leptoquark with fermion number $F = 2$. Diagrams involving a $F = 0$ leptoquark are obtained from (a) and (b) by exchanging q and $\bar{q}$.

lepton and a quark coming from the proton. This is illustrated in Fig. 1, where λ denotes the unknown Yukawa coupling of the LQ to the eq pair. Both these processes interfere with NC DIS. In contrast to [1] where both contributions and their interference with DIS were carefully taken into account in order to probe LQs masses close to or above the kinematic limit, we only consider here the resonant process. This approach is valid as long as the LQ mass M_{LQ} is not too high and its width $\Gamma \propto \lambda^2 M_{LQ}$ is small enough for the narrow-width approximation (NWA) to hold. In that case, the LQ mass spectrum is not distorted by the convolution of the

Breit-Wigner distribution characterizing the LQ resonance with the density in the proton of the incoming quark [1]. For $\sqrt{s_{ep}} = 320$ GeV, this is the case for LQ masses up to ~ 290 GeV when the strength of the Yukawa coupling is of the order of α_{EM}.

In the s-channel, a LQ is produced at a mass $M = \sqrt{s_{ep}x}$ where x is the momentum fraction of the proton carried by the struck quark. Scalar LQs produced in the s-channel decay isotropically in their rest frame leading to a flat $\mathrm{d}\sigma / \mathrm{d}y$ spectrum where $y = Q^2/s_{ep}x = \frac{1}{2}(1+\cos\theta^*)$ is the Bjorken scattering variable in DIS and θ^* is the decay polar angle of the lepton relative to the incident proton in the LQ centre of mass frame. In contrast, events resulting from the production and decay of vector LQs would be distributed according to $\mathrm{d}\sigma / \mathrm{d}y \propto (1-y)^2$. These y spectra (or in other words the specific angular distributions of the decay products) from scalar or vector LQ production are markedly different from the $\mathrm{d}\sigma / \mathrm{d}y \propto y^{-2}$ distribution expected at fixed x for the dominant t-channel photon exchange in neutral current DIS events. Hence, a LQ signal in the NC-like channel will be statistically most prominent at high y.

3 Event Selection and Comparison with SM Expectations

The search for first generation LQs relies essentially on an inclusive NC selection requiring an identified positron at high transverse energy. Selected events must have been accepted by a LAr trigger and survived a set of filters to reject non ep colliding background, and a primary vertex is required in the range $\mid z - \bar{z} \mid < 35$ cm.

3.1 Event Selection

The selection of NC-like events is identical to that presented in [1]. It mainly requires an isolated electron in the LAr with $E_{T,e} > 15$ GeV and an energy-momentum balance. A "loose" requirement of a jet in the LAr, with $P_{T,jet} > 7$ GeV, allows to suppress non-DIS contamination as $\gamma\gamma$ or QED Compton processes. The kinematic variables Q^2, M and y are determined using the measurement of the scattered electron energy and angle, the subscript e being used in the following to label the corresponding reconstructed variables.

The considered phase space is restricted to the kinematic range $Q^2_e > 2500$ GeV^2 and $0.1 < y_e < 0.9$. The resolution in M_e degrades with decreasing y_e ($\delta M_e/M_e \propto 1/y_e$) and so the low y domain is excluded. Excluding the high y values avoids the region where migrations effects due to QED radiation in the initial state are largest for the e-method, and also suppresses down to a negligible level the photoproduction background where e.g. a jet has been misidentified as an electron. In the kinematic range considered, the NC trigger efficiency exceeds 98% and is consistent with 100% to within experimental error.

Applying our NC selection criteria, 696 NC DIS candidates are observed in the considered kinematic range.

The distribution of these events in the $y_e - M_e$ kinematic plane is shown in Fig. 2. In this plane, events coming from a resonantly produced scalar LQ decaying to eq would accumulate in M_e around the LQ mass, and be flatly distributed in y.

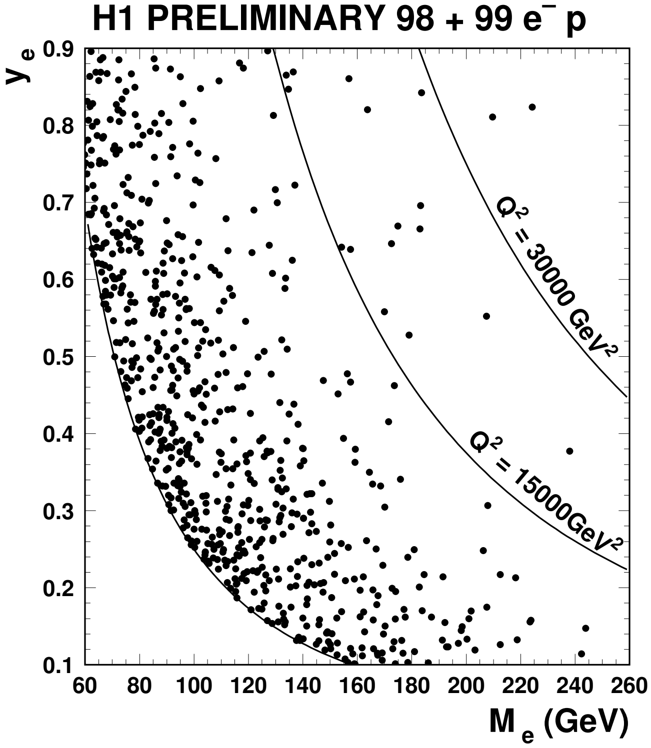

Figure 2: Kinematics in the $y_e - M_e$ plane of the selected NC DIS candidates. Three isocurves at $Q^2 = 2500, 15000$ and 30000 GeV^2 are also shown as full lines.

3.2 Comparison with NC DIS

The SM prediction for DIS is obtained using the event generator DJANGO [3] which includes QED first order radiative corrections and a modelling of the emission of QCD radiation to all orders according to the Color Dipole Model as implemented in ARIADNE [4]. The parton densities in the proton used throughout are taken from the MRST [5] parametrization which includes constraints from HERA data up to $Q^2 = 5000$ GeV^2.

The systematic errors propagated on the mean SM expectations include:

- the uncertainty on the integrated luminosity ($\pm 2.2\%$);
- the uncertainty on the absolute calibration of the calorimeters for electromagnetic energies, ranging between $\pm 0.7\%$ in the central LAr wheels to $\pm 3\%$ in the forward region of the LAr calorimeter;
- the uncertainty on the calibration of the calorimeters for hadronic showers of $\pm 2\%$;
- the uncertainty on the partons densities in the proton which lead to a 7% theoretical uncertainty on the predicted NC DIS cross-section.

Applying the requirements mentioned in section 3.1, 675.7 ± 50.6 events are expected from standard NC DIS, in good agreement with the number of observed candidates. Fig. 3 shows the distributions of the transverse energy of the electron $E_{T,e}$, its polar angle θ_e, the missing transverse momentum $P_{T,miss}$ and the transverse momentum $P_{T,jet}$ of the highest P_T jet, for the 696 observed candidates and for the NC DIS expectation. All distributions are seen to be well

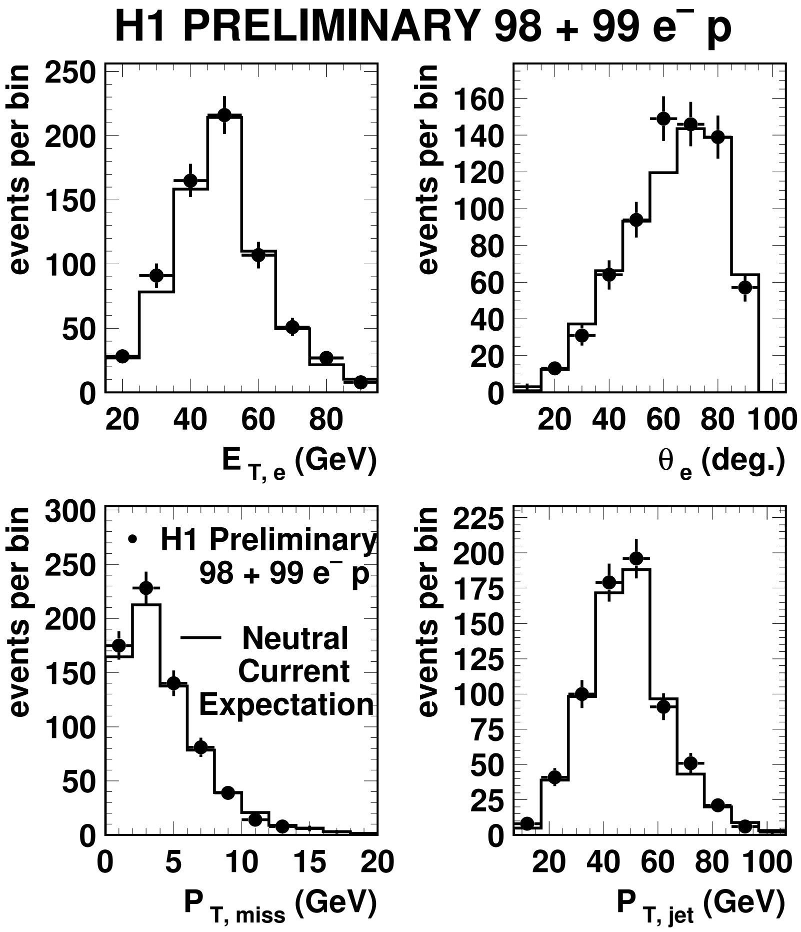

Figure 3: Distributions of (a) the transverse energy and (b) the polar angle of the electron; (c) the missing transverse momentum and (d) the transverse momentum of the highest P_T jet for the selected NC DIS candidates. Symbols correspond to data events and histograms to SM simulation.

described by the NC DIS simulation.

The observed and expected Q_e^2 distributions are compared in Fig. 4a. Also shown in Fig. 4b is the ratio of the observed Q_e^2 distribution to the NC DIS expectation. The errors resulting from the convolution of the systematic errors and the statistical error of the Monte Carlo sample are correlated for different Q_e^2 bins and are indicated in Fig. 4b as lines above and below unity joining the $\pm 1\sigma$ errors evaluated at the centre of each bin. The NC DIS expectation agrees well with the data, with a slight deficit observed for $Q_e^2 > 10000$ GeV^2 where 42 events are observed while 49.26 ± 5.18 are expected from SM expectation, which is however not statistically sig-

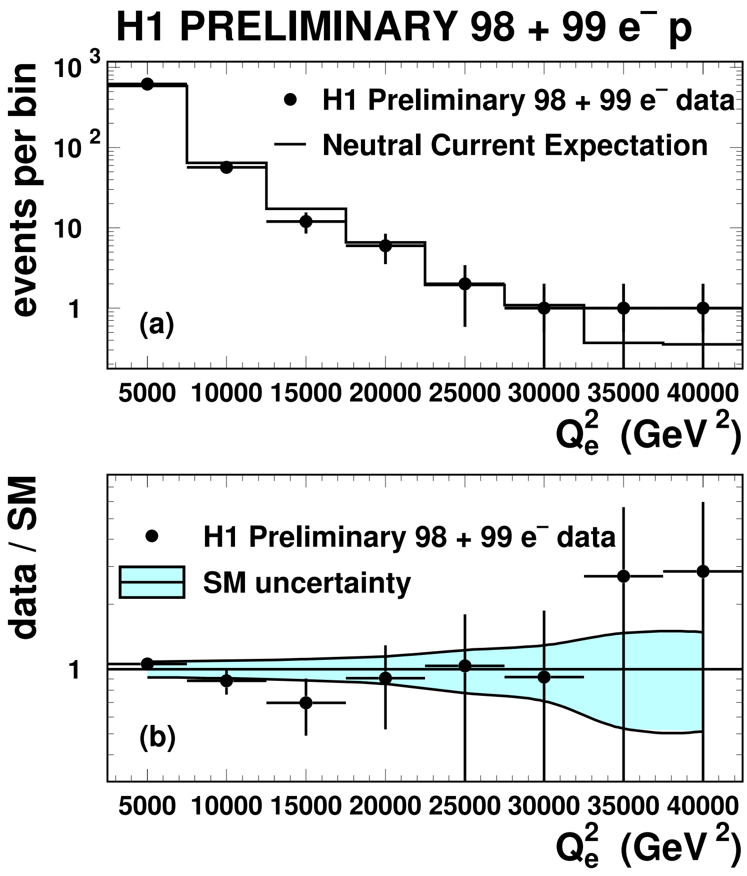

Figure 4: (a) Q_e^2 distribution of the selected NC DIS candidate events for the data (• symbols) and for standard NC DIS expectation (histogram); (b) ratio of the observed and expected (from NC DIS) number of events as a function of Q_e^2; the lines above and below unity specify the $\pm 1\sigma$ levels determined using the combination of statistical and systematic errors of the DIS expectation.

nificant. For $Q_e^2 > 15000$ GeV^2, 18 events are observed, in good agreement with the NC DIS prediction of 16.9 ± 2.43.

4 Direct Search for Leptoquarks

Starting from the NC DIS selection presented above, the significance of a possible LQ signal over the NC DIS background is enhanced by exploiting the specific angular distributions for LQ induced processes. The LEGO [6] event generator has been used to simulate events coming from the resonant production of scalar and vector LQs decaying into eq, for various values of the LQ mass M_{LQ}. For the LQ mass range considered here, the kinematics of events coming from $eq \to LQ \to eq$ does not depend on the value of the Yukawa coupling λ, provided that λ remains of moderate strength. These Monte-Carlo event samples have been used to optimize mass dependent lower $y_e > y_{cut}$ cuts which maximize the signal significance. This has been achieved by finding the best compromise between the efficiency loss on the LQ signal and the important background reduction. Thus, with increasing LQ mass, the y_{cut} decreases together with the NC DIS expectation. For scalar (vector) LQs, this y_{cut} continuously decreases from ∼0.45 (∼0.35) at 75 GeV to ∼0.35 (∼0.1) at 200 GeV, reaching 0.1 (0.1) at 290 GeV. The optimized y_{cut} is less stringent for vector than for scalar LQs due to the softer y distribution ($\propto (1-y)^2$) of events induced by vector LQ production.

4.1 Mass Distributions

The comparison of the measured mass spectrum with SM predictions is shown in Fig. 5 for the NC DIS analysis. The measured and expected NC spectra are seen before and after applying the mass dependent y_e cut relevant for the search of a scalar (Fig. 5a) and a vector (Fig. 5b) LQ. After applying the y_e cut optimized for scalar LQs, we observe 298 events in the mass range $M_e > 62.5$ GeV while 289.8 ± 21.8 are expected. For $M_e > 137.5$ GeV 21 candidate events are observed, which is slightly below the SM prediction of 29.8 ± 3.2. This is the reflection of the slight deficit observed above in the Q^2 distribution, for intermediate Q^2 values. The sample is less reduced when applying the y_e cut optimized for vector LQs searches, which leads to 514 candidates in good agreement with the 495.2 ± 37.2 expected from SM.

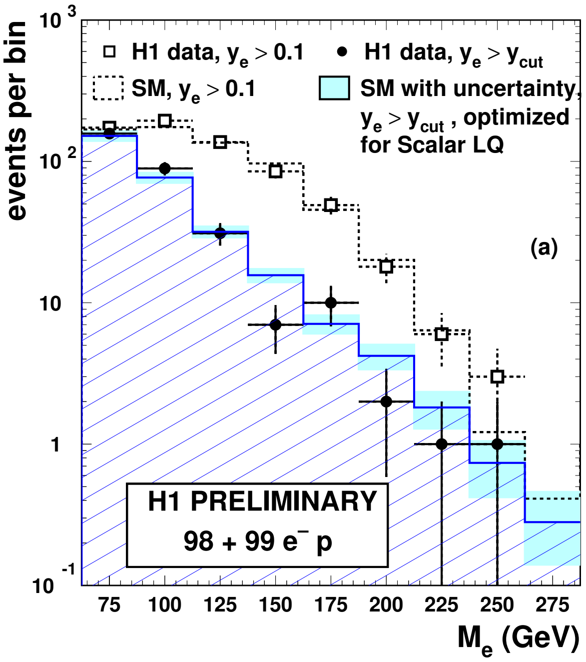

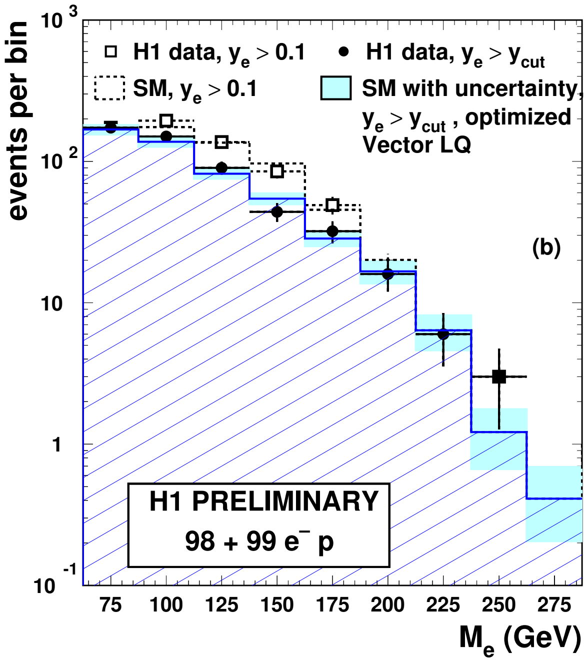

Figure 5: Mass spectra for NC DIS-like final states for data (symbols) and DIS expectation (histograms). The NC DIS-like comparison is shown before (open triangles, white histogram) and after (closed dots, hatched histogram) a y cut designed to maximize the significance of an eventual (a) scalar and (b) vector LQ signal. The greyed boxes indicate the $\pm 1\sigma$ band combining the statistical and systematic errors of the NC DIS expectation.

4.2 Constraints on LQs

Since no evidence for LQ production is observed, the data is used to set constraints on LQs coupling to first generation fermions.

For a given LQ mass, we use the numbers of observed and expected events within a mass bin $[M_{min}, M_{max}]$ of variable width, adapted to the expected mass resolution (typically $3-6$ GeV, dominated by experimental effects) and measured mass values for a given true LQ mass, and which slides over the accessible mass range. For example, only candidates with $M_e \in [187; 206]$ GeV will be used to constrain a 200 GeV LQ undergoing a NC DIS-like decay. In the mass domain where the NWA holds, M_{min} and M_{max} vary linearly with the LQ mass. Typical detection efficiencies of scalar (vector) LQs including the optimized y and mass cuts are found to vary between 35% (18%) at 100 GeV, 40% (45%) at 200 GeV and 52% (45%) at 290 GeV.

Assuming Poisson distributions for the SM background expectation and for the signal, an upper limit on the number of events coming from LQ production is then obtained using a standard Bayesian prescription with a flat prior for the signal cross section. The procedure which folds in the statistical and systematic errors is described in detail in [2]. This number can be translated into a limit on the product $\sigma_{LQ}\beta_e$ of the LQ production cross section σ_{LQ} and the branching ratio β_e for the LQ to decay into eq. NLO QCD corrections to σ_{LQ} were calculated in [7] and are taken into account here. They lead to an enhancement of the LQ cross section by $15\% - 30\%$ for LQ masses between 100 GeV and 290 GeV. In the NWA, σ_{LQ} scales with the square of the Yukawa coupling, hence upper limits on $\lambda\sqrt{\beta_e}$ are obtained as a function of the LQ mass. Thus, assuming a specific LQ model (e.g. [8]) in which β_e is known, mass dependent upper limits on λ can be derived. On the other hand, assuming a given value for the coupling λ, limits on the branching ratio β_e can be obtained as a function of the LQ mass. These two approaches are addressed in the following.

4.2.1 Limits on the Yukawa coupling in the BRW model

The phenomenological model proposed by Buchmüller-Rückl-Wyler (BRW) [8] describes 14 LQs, half of them having a fermion number $F = 2$, i.e. coupling to $e^- + q$. We focus on those LQs since LQs with $F = 0$ are better constrained using e^+p data [1]. In the BRW model the branchings β_e are fixed and equal to 1 or 0.5 depending on the LQ type. In this framework, mass dependent upper limits on the Yukawa coupling can then be set for each LQ type. These limits are represented in Fig. 6. Those limits considerably extend the domain excluded by the analysis of e^+p data [1], represented as the most upper curve on each plot. For Yukawa coupling of the electromagnetic strength ($\lambda = 0.3$) LQ masses up to 290 GeV are excluded at 95% confidence level (CL). For such LQ mass and coupling, the NWA is still valid within $\sim 30\%$ and the interference of LQ production with NC DIS remains below 1% of the LQ resonant production cross section in the kinematic domain where the signal is searched for, which justifies the approximation made in the analysis.

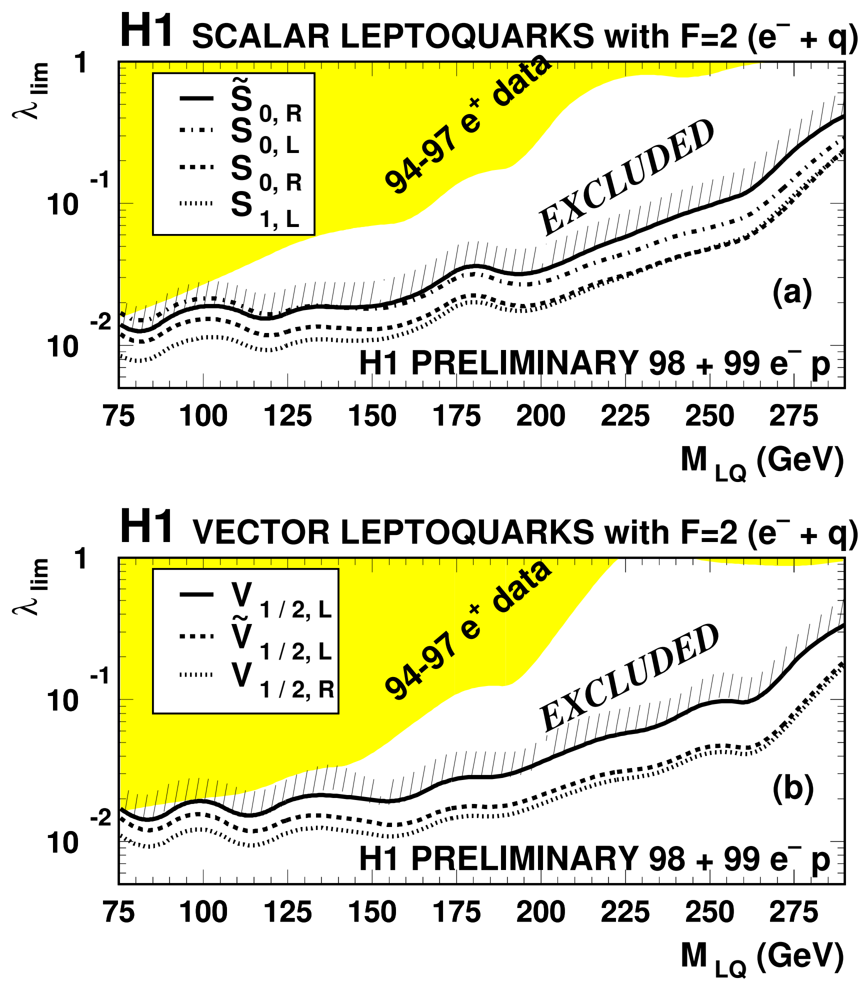

Figure 6: Exclusion limits at 95% CL on the Yukawa coupling λ as a function of the LQ mass for (a) scalar and (b) vector LQs with fermion number $F = 2$ described by the BRW model. Domains above the curves are excluded. The upper curve on each plot indicates the limit obtained from the (less suited for $F = 2$ LQs) e^+p data [1].

4.2.2 Mass Dependent Limits on $\beta(LQ \to eq)$

Moving away from the BRW model, we now consider leptoquarks which undergo NC DIS-like decays with a branching ratio β_e and do not make any assumption on the other possible decay modes of the LQ. For a fixed value of the Yukawa coupling λ upper limits on β_e are derived as shown in Fig. 7a and Fig. 7b for a $F = 2$ scalar LQ coupling to e^-d and e^-u respectively. It can be seen that the domain excluded by this analysis extends considerably beyond the region excluded by the $D\emptyset$ experiment at the TeVatron, represented as the hatched domain on Fig. 7.

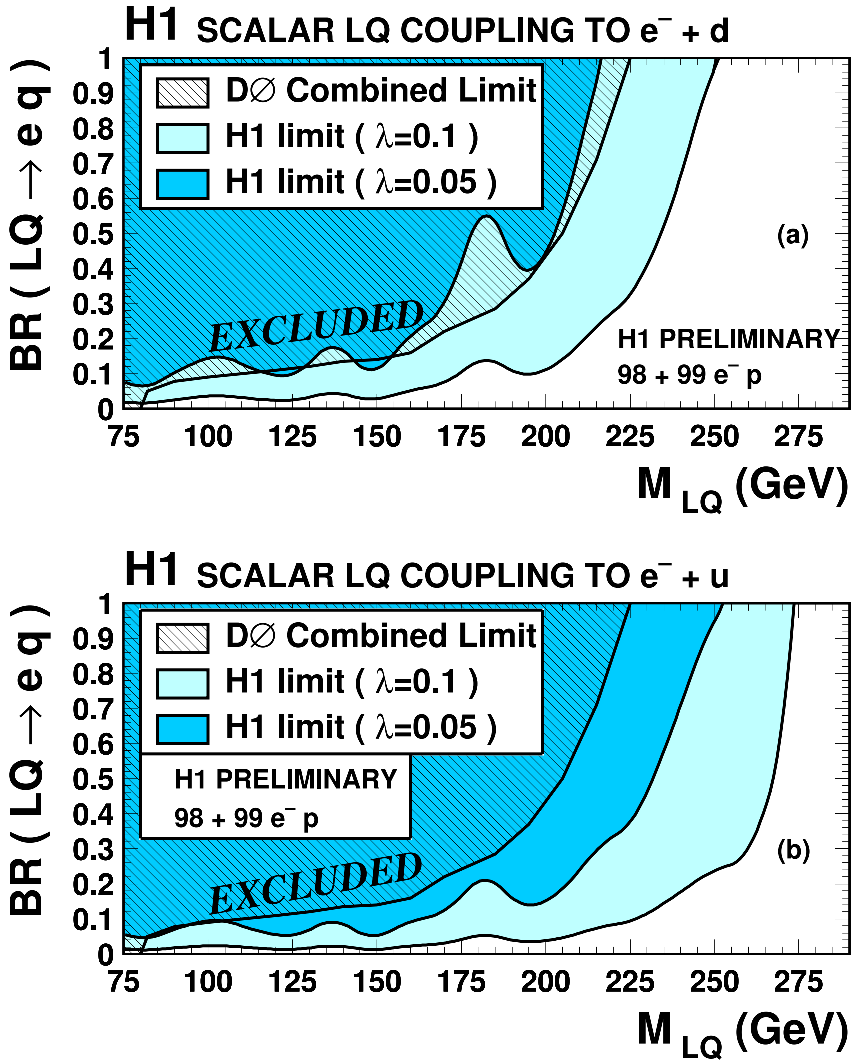

Figure 7: Mass dependent exclusion limits at 95% CL on the branching ratio β_e of the LQ to decay into eq for scalar LQs with $F = 2$ produced by (a) e^-d and (b) e^-u fusion. The $D\emptyset$ limit is also shown as hatched region.

5 Conclusions

Leptoquarks with fermion number $F = 2$ have been searched using the e^-p data collected by H1 in 1998 and 1999. No signal has been observed and constraints on such LQs have been set, allowing to extend beyond the domains excluded by other experiments. Moreover the constraints set here on $F = 2$ LQs are more stringent than those on $F = 0$ LQs obtained in [1] from the higher statistics e^+p data sample, due to the enhanced energy in the centre of mass of the ep collision.

References

[1] H1 Collaboration, C. Adloff *et al.*, Eur.Phys.J. C11 (1999) 447.

[2] H1 Collaboration, T. Ahmed *et al.*, Z. Phys. C64 (1994) 545.

[3] DJANGO 6.2; G.A. Schuler and H. Spiesberger, Proc. of the Workshop Physics at HERA, W. Buchmüller and G. Ingelman (Editors), (October 1991, DESY-Hamburg) Vol. 3 p. 1419.

[4] ARIADNE 4.08; L. Lönnblad, Comput. Phys. Commun. 71 (1992) 15.

[5] A.D. Martin, R.G. Roberts, W.J. Stirling and R.S. Thorne, Euro. Phys. J. C4 (1998) 463.

[6] LEGO 0.02 and SUSSEX 1.5; K. Rosenbauer, dissertation RWTH Aachen (in German), PITHA 95/16, July 1995.

[7] T. Plehn *et al.*, Z. Phys. C74 (1997) 611.

[8] W. Buchmüller, R. Rückl and D. Wyler, Phys. Lett. B191 (1987) 442. *Erratum* Phys. Lett. B448 (1999) 320.